IOPscience iopscience.iop.org

Home Search Collections Journals About Contact us My IOPscience

Performance of the lithium metal infused trenches in the magnum PSI linear plasma simulator

This content has been downloaded from IOPscience. Please scroll down to see the full text.

2015 Nucl. Fusion 55 113004

(http://iopscience.iop.org/0029-5515/55/11/113004)

View the table of contents for this issue, or go to the journal homepage for more

Download details:

IP Address: 128.174.163.129
This content was downloaded on 25/01/2016 at 15:56

Please note that terms and conditions apply.

IOP Publishing | International Atomic Energy Agency Nuclear Fusion

Nucl. Fusion **55** (2015) 113004 (8pp) doi:10.1088/0029-5515/55/11/113004

Performance of the lithium metal infused trenches in the magnum PSI linear plasma simulator

P. Fiflis[1], T.W. Morgan[2], S. Brons[2], G.G. Van Eden[2], M.A. Van Den Berg[2], W. Xu[1], D. Curreli[1] and D.N. Ruzic[1]

[1] Center for Plasma Material Interactions, Department of Nuclear, Plasma and Radiological Engineering, University Illinois at Urbana-Champaign, Urbana, IL 61801, USA
[2] FOM Institute DIFFER-Dutch Institute For Fundamental Energy Research, Association EURATOM-ROM, Trilateral Euregio Cluster, 5612, Nieuwegein, The Netherlands

E-mail: fiflis1@illinois.edu

Received 20 April 2015, revised 6 August 2015
Accepted for publication 10 August 2015
Published 4 September 2015

Abstract

The application of liquid metal, especially liquid lithium, as a plasma facing component (PFC) has the capacity to offer a strong alternative to solid PFCs by reducing damage concerns and enhancing plasma performance. The liquid-metal infused trenches (LiMIT) concept is a liquid metal divertor alternative which employs thermoelectric current from either plasma or external heating in tandem with the toroidal field to self-propel liquid lithium through a series of trenches. LiMIT was tested in the linear plasma simulator, Magnum PSI, at heat fluxes of up to 3 MW m^{-2}. Results of these experiments, including velocity and temperature measurements, as well as power handling considerations are discussed, focusing on the 80 shots performed at Magnum scanning magnetic fields and heat fluxes up to ~0.3 T and 3 MW m^{-2}. Comparisons to predictions, both analytical and modelled, are made and show good agreement. Concerns over MHD droplet ejection are additionally addressed.

Keywords: divertor, lithium, liquid metal

(Some figures may appear in colour only in the online journal)

Introduction

The employment of liquid lithium offers many benefits as a plasma facing component in magnetic confinement devices. Low core impurity concentrations [1], more stable plasmas [1, 2], and improvements in energy confinement time [3] are merely some of these, however, fueling rates would probably need to be increased to maintain plasma density [4]. Literature shows that lithium causes a reduction in Zeff of the plasma [5, 6]. NSTX has seen broadened plasma pressure profiles, leading to higher beta stability for high performance H-mode discharges when using lithium [7]. The same study also found a 50% reduction in peak heat load on the liquid lithium divertor which was attributed to enhanced divertor bolometric radiation. A recent study at D-IIID found that use of lithium contributed to a long ELM free period without significant increase of core impurities with a more robust pedestal (attributed to a bursty-chirping mode (BCM)) and increased H98 (~1.5) [8]. Lithium also does not accumulate in the core [9]. The most important benefit of liquid lithium however, may be its durability as a divertor material. Solid divertors, such as the tungsten monoblock design for ITER, suffer from erosion by sputtering and off normal events, blister and fuzz formation, and in extreme cases, melt damage. Liquid lithium, however, suffers from only erosion, but the eroded material is easily replaced as additional lithium flows into the device. A liquid lithium divertor concept, LiMIT [10], has been designed and tested at Illinois. LiMIT uses thermoelectric magnetohydrodynamic (TEMHD) flow [11, 12] to self-propel lithium down a series of trenches, employing lithium as both a plasma facing surface and a coolant. TEMHD flow relies on a thermal gradient to drive thermoelectric currents

 © 2015 IAEA, Vienna Printed in the UK

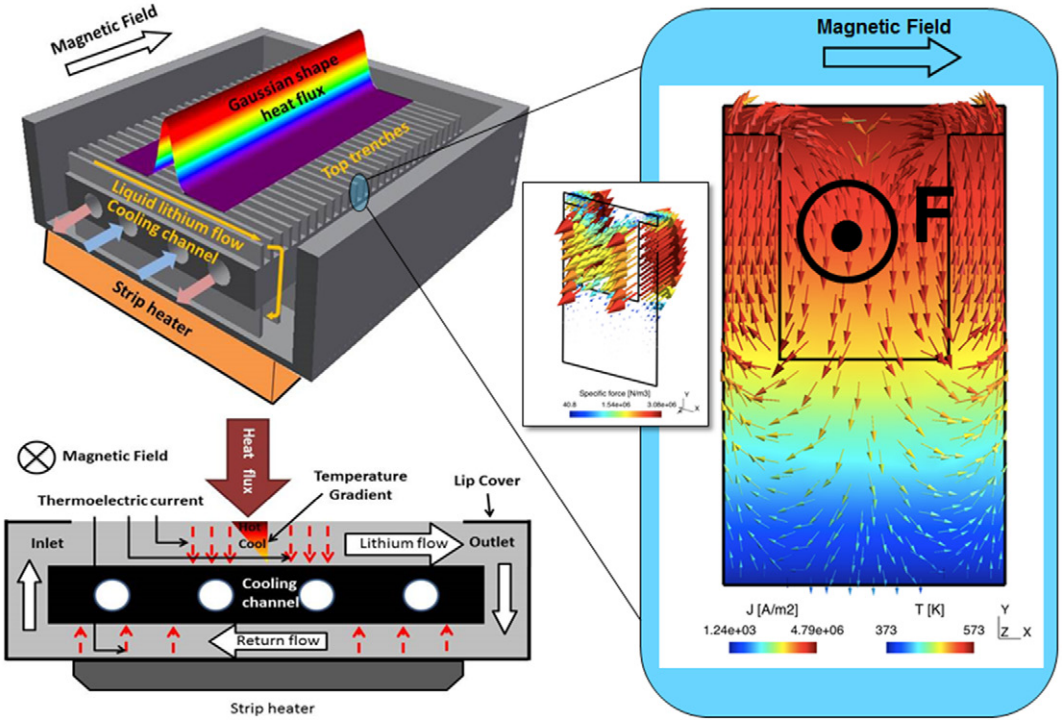

Figure 1. Illustration of thermoelectric magnetohydrodynamic effect showing heating of one side of the trenches combined with cooling of the other side (top left) gives rise to thermoelectric currents in the lithium and trench walls (right, generated via 2D thermoelectric GetDP simulation) which combined with a magnetic field gives rise to lithium flow (bottom left).

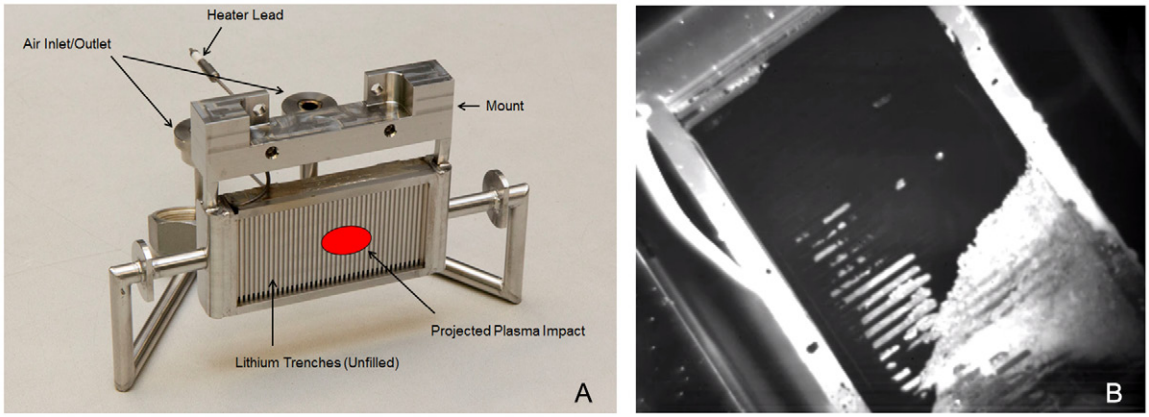

Figure 2. Stainless steel trenches employed in tests on Magnum PSI. Trenches in A (left) are unfilled, but illustrate projected plasma strike point, mounting strut and coolant connections. Trenches in B (right) are filled and inserted into exposure chamber. Plasma impingement direction is from the lower right. Module body (made of stainless steel, white on IR image) can be seen as well as lithium fill (dark on IR image) and passivated lithium layers (upper left on trench structure, light on IR image). It can be seen that a very thin layer of lithium covers the tops of the stainless steel trenches, so that the entire PFC surface is lithium.

that then interact with a magnetic field to drive flow; in the case of a tokamak this magnetic field would be the main toroidal field. Plasma heating of the surface combined with cooling at the bottom of the LiMIT trenches provides the thermal gradient, a schematic can be seen in figure 1. LiMIT has undergone significant testing in the SLiDE facility at Illinois [10, 13], as well as a test on the HT-7 tokamak [14]. To further develop the design's viability as an alternative to tungsten PFCs, exposure of a LiMIT test module to sustained large heat and particle fluxes was performed at the Magnum PSI linear plasma simulator.

Experimental setup

The experimental setup consists of a series of air-cooled stainless steel trenches, hereafter referred to as the tray, mounted on the main target manipulator of the Magnum PSI linear simulator [15]. A photo of the tray can be seen in figure 2(*A*). The lithium channels in the design were 1 mm wide by 2 mm deep by 5 cm long on the top side. Filling of the device with lithium was accomplished in vacuum by heating the tray to 475 °C and using a lithium injector similar to that used in wetting experiments at Illinois [16] to introduce lithium into

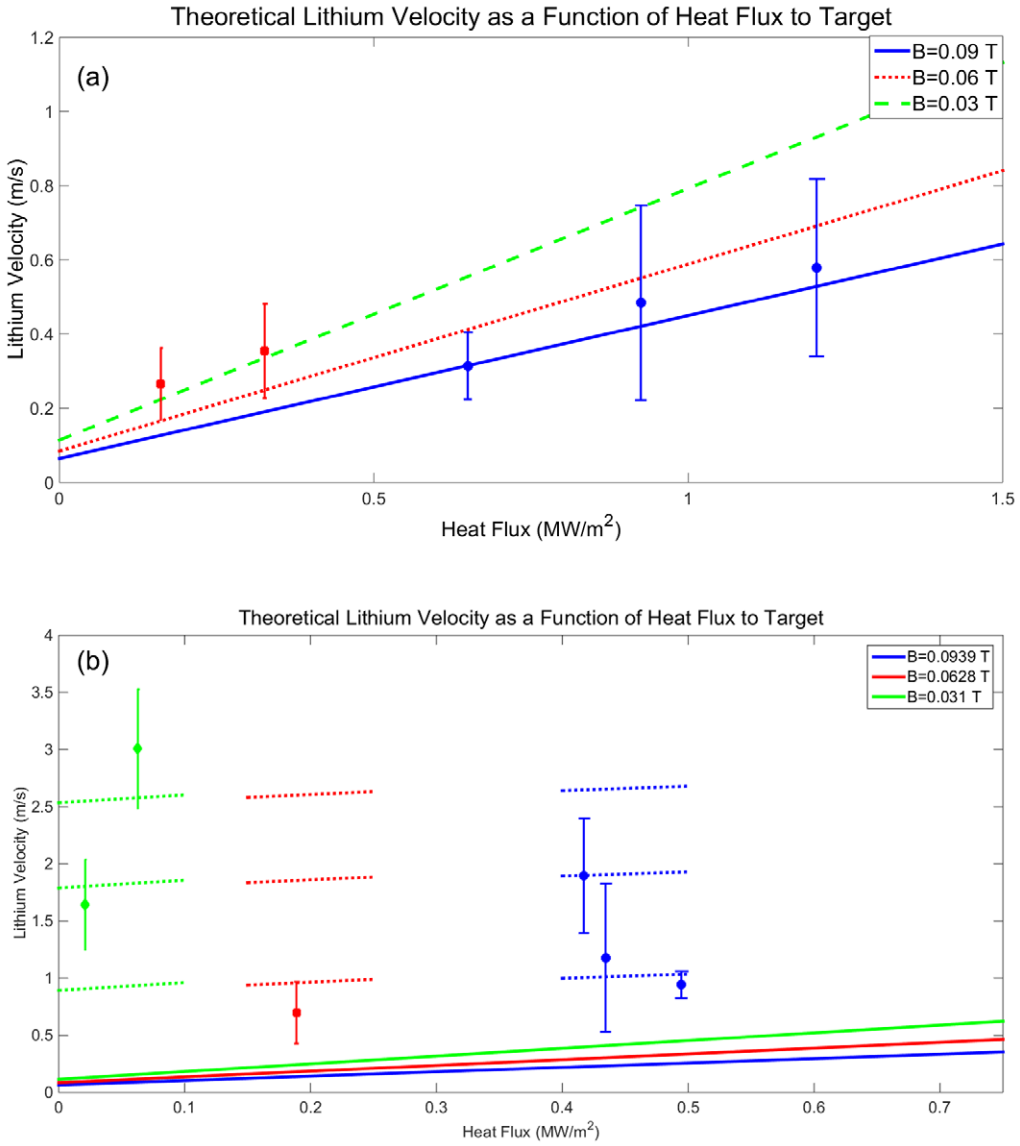

Figure 3. (*A*) Well characterized lithium velocity measurements in the LiMIT structure showing good agreement between theory and experiment. (*B*) Several single shot lithium velocity measurements showing greater experimentally determined velocity than theoretically predicted. Discrepancy attributed to capillary/gravity waves on the surface. Additional dotted lines show sum of predicted lithium velocity and phase velocities of waves.

the tray. The magnetic fields explored were relatively low (order of 0.1 T), however, previous studies have investigated the performance of LiMIT under larger magnetic fields [10, 14]. Resistive heaters were placed on the sides and bottom of the tray to achieve the 475 °C temperature, as well as to provide a thermal gradient to drive TEMHD flow in the return channels of the LiMIT device. Though the contact angle of the lithium on the stainless steel was significantly less than 90°, wicking into the trenches was only accomplished via the use of an agitator to break the surface tension of the injected lithium pool, which then flowed into the channels and filled the tray. A filled picture of the tray can be seen in figure 2(*B*). It has been shown that when lithium wets a surface, it does not unwet [16]. Likewise, the LiMIT trenches stayed wetted for the entirety of the tests performed. Once filled, the tray was moved from the target exchange chamber into the exposure chamber. Once in the exposure chamber, the tray was exposed to helium, hydrogen, and argon plasmas at several different magnetic fields and heat fluxes. The LiMIT device was diagnosed by a fast frame visible camera (Phantom V12), maximum frame rate 1 MHz (operated between 1000 and 10 000 Hz), a fast frame IR camera (FLIR SC7500MB), maximum frame rate 30 kHz (operated between 300 and 1000 Hz), as well as a thermocouple and an IR pyrometer (Far Associates FMPI SpectroPyrometer).

Lithium velocity results

The velocity of the liquid lithium was most readily characterized via the fast frame IR camera. The velocity was determined by tracking the velocity of impurities entrained in the lithium flow. The IR emissivity of lithium is much lower than that of the lithium oxides, hydroxides, and nitrides that form

on the lithium surface. When these impurity layers are broken and entrained in the flow, an estimate of the lithium velocity can be obtained from the velocity of the impurity. The velocity of the impurities was derived from its frame to frame displacement, compared to the total trench length, divided by the frame rate. Theoretically, the velocity is determined by a balance between TEMHD drive and MHD damping of the flow [10]. The TEMHD driven velocity of a square duct of lithium has been derived by Shercliff [11] for a constant temperature gradient. Equating the velocities for the unheated and heated sections of the lithium channel leads to the following relation:

$$u_m = \frac{\frac{S}{B}\left(\frac{Q_{\mathrm{ohm}}}{k+2\rho c_p\left(\frac{1}{2}h_{\mathrm{O}}^2 w\right)\frac{u_m}{L_{\mathrm{O}}}} + \frac{L_P}{L_O}\frac{(1+c_{\mathrm{O}})}{(1+c_{\mathrm{P}})}\frac{Q_{\mathrm{plasma}}}{\left(k+\rho c_p\left(\frac{1}{2}h_{\mathrm{P}}^2\right)\frac{u_m}{L_P}\right)}\right)}{\frac{Ha+c_{\mathrm{O}}\tanh(Ha)}{2HaX} + \frac{(1+c_{\mathrm{O}})}{L_{\mathrm{O}}X}(L_{\mathrm{U}}) + \frac{L_{\mathrm{P}}}{L_{\mathrm{O}}}\frac{(1+c_{\mathrm{O}})}{(1+c_{\mathrm{P}})}\frac{Ha+c_{\mathrm{P}}\tanh(Ha)}{HaX}},$$

$$c_x = \frac{w\sigma}{t\sigma_w},\ X = 1 - \frac{\tanh(Ha)}{Ha}$$

Where the mean velocity is dependent on S, the relative thermopower between the lithium and trench material, B, the magnetic field, Ha, the Hartmann number of the flow, k, ρ, and c_p, respectively the thermal conductivity, density, and specific heat of the lithium, c_x the weighted ratio of lithium to wall conductivity, as well as the unheated, ohmically heated, and plasma heated lengths, L_{U}, L_{O}, and L_{P}. A series of comparison graphs each containing different data sets illustrate the experimentally obtained velocity results versus the theoretically predicted velocity in figures 3(*A*) and (*B*), showing good agreement with theory for well characterized (multiple shot) magnetic field and heat flux points (3*A*). The IR images resulting in these velocity determinations have a very clearly defined impurity particle travelling along the surface. Other observed motions on the surface show a streak, rather than a clearly defined particle in the IR image and there is a significant deviation in these cases between the theory and experiment (3*B*). The experimentally determined velocity is typically 0.5–2 m s^{-1} faster than theoretically predicted. This is hypothesized to be due to the presence of capillary/gravity waves increasing the apparent surface velocity. The streak observed is indicative of a change in surface height from a wave travelling along the channel rather than a small impurity. The dispersion relation for low amplitude, shallow gravity/capillary waves is given by [17]:

$$\omega^2 = \left(gk + \frac{\gamma k^3}{\rho}\right)\tanh(kh)$$

Where ω is the frequency, k the wavenumber, γ the surface tension, ρ the density, and h the channel height. Clearly identifiable surface waves have been observed in IR videos to be travelling at 1.6–2 m s^{-1} (see figure 4). Further analysis was performed on the IR videos to determine the dominant wavenumbers of the observed travelling wavepackets. The IR intensity as a function of pixel number and frame was examined for the frames containing the travelling wavepackets along a single trench. Plotting the IR intensity versus distance along the trench, and subsequently taking a Fast Fourier Transform

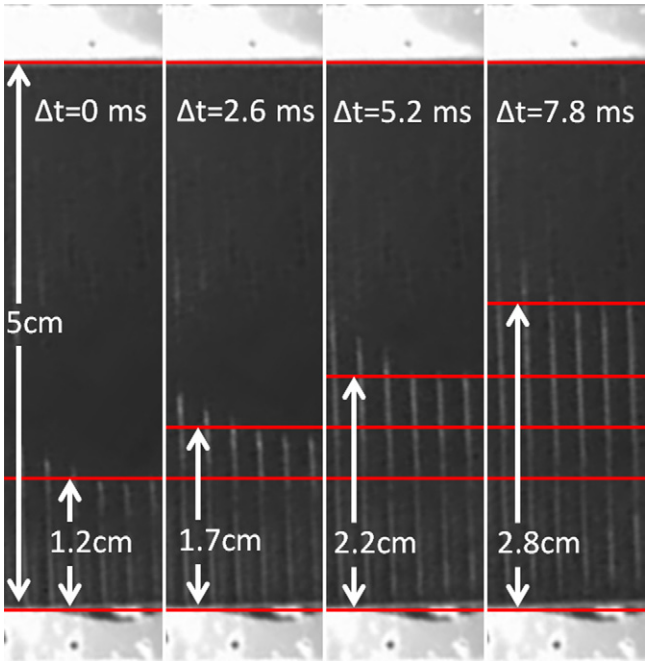

Figure 4. Series of successive frames from infrared camera (Shot 65) showing surface wave travelling along the lithium. Velocity of wave is determined from wavefront displacement per frame times frame rate (IR frame rate = 383 frames s^{-1} for shot 65). Wave can be seen in fast frame IR video to travel length of trench several times, reflecting at the sides of the LiMIT structure.

for each of the frames yielded two dominant wavenumbers (k = 4.5e3 m^{-1} and k = 9.42e3 m^{-1}) and a third less dominant wavenumber (k = 1.05e3 m^{-1}) for the wavepackets. The corresponding phase velocities of these wavenumbers are 1.67, 2.42, and 0.78 m s^{-1} respectively. Dotted lines representing the sum of the predicted lithium velocity and the dominant wavenumber phase velocities are shown in figure 3(*B*) illustrating agreement between the observed experimental velocities and predicted dominant wavenumber velocities.

LiMIT thermal response

The surface temperature was tracked with the IR camera and a correlation was made between the surface temperature rise and the impinging heat flux parallel to the beam. Surface temperatures recorded from the infrared camera are calibrated for each shot by comparison with the thermocouple. The resulting change in surface temperature at the beam-spot center (δT) for each shot is plotted in figure 5 against the parallel heat flux. Two trends are obvious, one following the δT from exposure at 75° to the beam and the other at 45° to the beam. A fit to δT versus incident heat flux is linear, indicating that the dominant heat transfer mechanisms for the tests performed were convection and conduction rather than radiation, which is readily supported by a simple order of magnitude comparison. The fits also have a nonzero intercept, indicative of hotter lithium being transported to the top surface from the back channels. Since heaters are only in direct contact with the return portion of the channels and not with the plasma facing portion, lithium in the return side is hotter. Even with zero heat flux

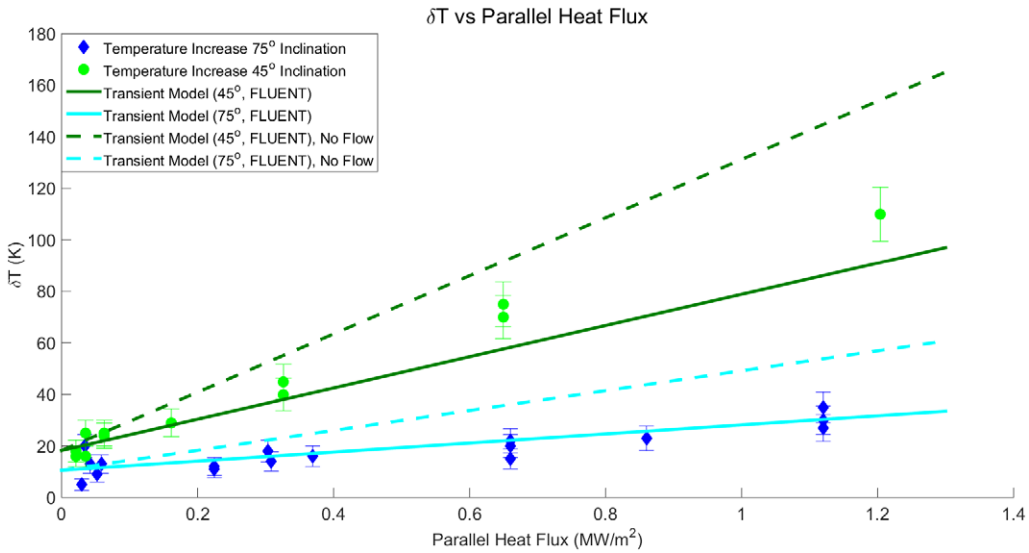

Figure 5. Change in lithium surface temperature versus parallel heat flux showing data (diamonds, best fit line), 3D transient thermal model (solid line), and 3D transient thermal model in the absence of lithium velocity (dotted line).

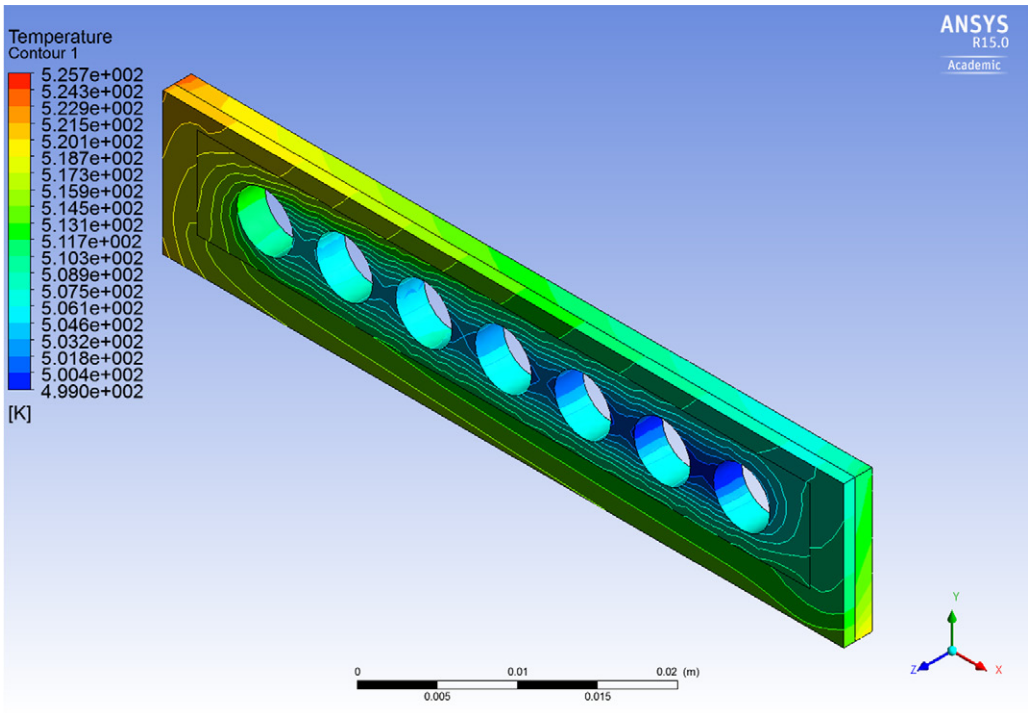

Figure 6. 3D thermal model computational domain showing cooling channels, Li channel (forward), and stainless steel structural trench (rear). ½ of a trench is modeled.

to the plasma facing area, application of a magnetic field will cause hotter lithium to circulate from the return portion to the plasma facing portion, causing the temperature of the lithium locally at the point of measurement to increase. A linear fit is also suggestive of a lack of vapor shielding [18], which would only become dominant at large temperatures (>400 °C) as the evaporative flux of lithium from the target increases and a vapor cloud is formed. For the shots during which the IR camera did not saturate, the temperature was too low for vapor shielding [19]. This is verified by analysis of fast frame visible camera data. The camera was equipped with a Lithium I filter (Andover, 3 nm FWHM). The counts on the camera were recorded to analyze the vapor shielding properties of the surface. The integrated power emitted from vapor shielding, approximately $P = \frac{4\pi E_p \Phi}{\Omega}$, energy per photon times photon flux to the camera divided by the solid angle subtended by the camera is much less than the power input from the heaters and the plasma. Two further observations can be gleaned from a comparison of the data with a 3D time-dependent heat transfer simulation. A single half-trench (both lithium and the structural stainless steel) was modeled in the finite-volume solver FLUENT [20], the computational domain can be seen

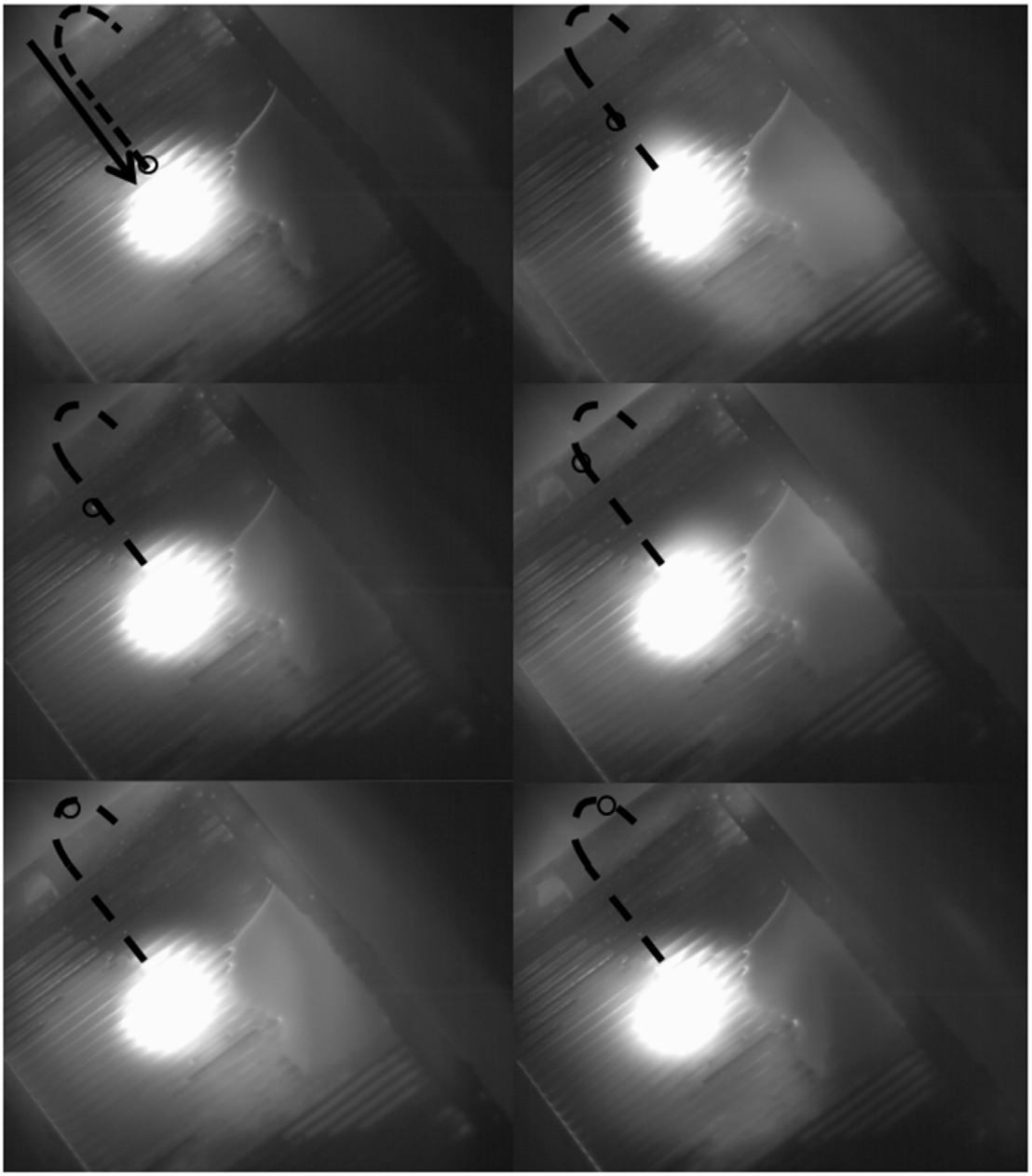

Figure 7. Series of frames showing the expulsion and subsequent entrainment of a lithium droplet in the plasma flow. Dashed line shows path of lithium droplet, circles illustrate droplet position, solid arrow is direction of plasma flow.

in figure 6. Each shot from which a δT was drawn from the IR data was analyzed with the model. The velocity of the lithium in the top of the channels was set to the theoretically predicted velocity for the shot (as predicted by the momentum balance of the previous section). The boundary conditions for the heat fluxes are as follows: the side walls and the bottom were a uniform heat flux equal to that provided by the resistive heaters in the experiment. The center boundary condition to each of the coolant channels was a convective boundary condition into air at room temperature, where the heat transfer coefficient was adjusted such that in the absence of a heat flux on the top surface, the temperature of the top of the structure equilibrated at 230 °C; which is the average starting temperature of the LiMIT trenches before the shot. For each of the time dependent simulations, the solver was initialized to this steady state condition. At time $t = 0$, for each shot, a Gaussian heat flux, of peak intensity equal to the peak intensity as measured by Thomson scattering of the beam, for each set of shot conditions, was applied to the top of the device for a duration equal to the shot length. The average change in temperature of the top surface was then calculated using the solver. The model results are co-plotted with the data in figure 5. Each simulation was then re-run employing zero lithium velocity to contrast the effect of lithium flow with the corresponding no flow case. From this, a series of observations can be made. First, the temperature increase in the channels is much lower than would be expected if there was no lithium flow. Second, the 75° δT model results and experimental data are well correlated, providing strong evidence that conduction and convection are the dominant mechanisms. Finally, the 45° δT experimental

results lie above the computational curve, yet below the zero velocity case. The authors posit that this is due to plasma pressure depressing the layer of lithium in the higher tilting angle cases and reducing the amount of lithium available to conduct and convect away heat, resulting in higher δT.

Lithium droplet emission

One of the main concerns over liquid lithium divertors is the expulsion of lithium droplets from the surface under intense plasma exposure. It was hypothesized that the small width of the trenches in tandem with the high surface tension of the liquid lithium would contribute to reducing the emission of lithium from the surface. Droplet expulsion was tracked using the fast frame visible camera. A significant reduction was noted in comparison to previous tests performed on pools of liquid metal [21], with the droplets emitted being emitted from lithium not constrained by trenches (due to overfill). A quick analysis using linear stability theory, with surface tension maintaining the surface and JxB forces causing perturbation, as implemented by Jaworski *et al* [22], shows that for the 1 mm trenches used, at the maximum magnetic field employed, a current density of 58 MA m^{-2} would be necessary to eject droplets which is much greater than can be achieved in Magnum PSI (order of 1e5 A m^{-2}) [23]. Lithium emission from the trenches was nearly nonexistent (less than 10 droplets observed to be emitted from trench structures in over 70 shots). Almost all of the lithium droplets were entrained in the plasma flow, in several cases leading to re-deposition in the tray. Figure 7 shows a series of frames illustrating emission of a lithium droplet followed by entrainment and redeposition.

Discussion and summary

LiMIT was exposed to a series of 73 shots in the linear plasma device, Magnum PSI. Averaged velocity measurements are in good agreement with theoretical predictions delivered by a 0D momentum balance. Lithium velocity measurements not in agreement with the theoretical predictions are thought to be a result of capillary/gravity waves on the surface of the lithium. Improved velocity diagnostics will be pursued in future experiments to more accurately determine the total flowrate of lithium and decouple the effect of capillary/gravity waves. IR camera measurements of the thermal response of the LiMIT system show a linear trend of temperature rise with heat flux, indicative of conduction and convection, not vapor shielding or radiation, being the main heat transfer mechanisms in the tests here. A 3D transient thermal model shows good agreement with the δT in the 75° inclination tests. The 45° inclination δT is underpredicted by the model, which is thought to be due to thinning of the lithium channel due to plasma exposure. Lithium droplet emission was greatly decreased from the open lithium pool case by surface tension of the lithium in the narrow channels. Ultimately, the air-cooled stainless steel LiMIT structure suffered a partial melt under exposure to a 3 MW m^{-2} plasma. In this shot, plasma pressure and a high lithium velocity cooperated to cause a large buildup of lithium on the downstream side of the plasma spot. The lithium buildup was higher than the wall, causing leakage over the edge. Only after a significant amount of leakage was the lithium no longer to take the heat away from the point of impact, and at this point the stainless steel underwent a local partial melt. Had lithium remained, the FLUENT model of the thermal response section of this paper predicts a temperature rise of 180 °C (ultimate temperature of 435 °C), which is not enough to melt the steel. In the higher heat flux tests, it was noticed that the thickness of the lithium directly under the plasma strike point was thinner than the areas not under the plasma spot. This is attributed to an increased driving force directly under the plasma strike point. While lithium moving out from this point is continually replaced by lithium pulled from the inlet, conservation of lithium flowrate dictates that because of the increased velocity, the lithium cross section decreases, and therefore the lithium layer thins. Two potential solutions have been proposed to address this concern, namely adjusting the trench dimensions at this point to a smaller cross sectional area so that the lithium thickness does not decrease, or by inclusion of a wire mesh over the top of the trenches to maintain the surface height by surface tension. Future studies will investigate the viability of these proposed solutions. These tests provide confirmation of the underlying physics of the LiMIT concept, enabling design of a more robust iteration of this alternative divertor concept. The next design will look to include larger return flow channels and wire mesh in order to mitigate the pileup of lithium.

Acknowledgments

This work was performed under US DOE Grants DEFG02-99ER54515 and DE-FOA-0000603. The work was performed at the Magnum PSI linear plasma simulator in Nieuwegein, Netherlands.

References

[1] Mazzitelli G. *et al* 2010 Review of FTU results with the liquid lithium limiter *Fusion Eng. Des.* **85** 896
[2] Zuo G.S. *et al* 2011 Study on H-mode access at low density with lower hybrid current drive and lithium-wall coatings on the EAST superconducting tokamak *Nucl. Fusion* **51** 072001
[3] Majeski R., Doerner R., Gray T., Kaita R., Mansfield D., Spaleta J., Soukhanovskii V., Timberlake J. and Zakharov L. 2006 Enhanced energy confinement and performance in a low-recycling tokamak *Phys. Rev. Lett.* **97** 075002
[4] Majeski R., Doerner R., Gray T., Kaita R., Maingi R., Mansfield D., Spaleta J., Soukhanovskii V., Timberlake J. and Zakharov L. 2006 Enhanced energy confinement and performance in a low-recycling tokamak *Phys. Rev. Lett.* **97** 075002
[5] Mirnov S. *et al* 2006 Experiments with lithium limiter on T-11M tokamak and applications of the lithium capillary-pore system in future fusion reactor devices *Plasma Phys. Control. Fusion* **48** 821
[6] Chen Y. *et al* 2015 Investigations of Z_{eff} and impurity behavior in lithium coating experiments with full metallic first wall in HT-7 tokamak *Plasma Phys. Control. Fusion* **57** 025012

[7] Ono M. *et al* 2013 Recent progress in the NSTX/NSTX-U lithium programme and prospects for a reactor-relevant liquid-lithium based divertor development *Nucl. Fusion* **53** 113030
[8] Osborne T.H. *et al* 2015 Enhanced H-Mode pedestals with lithium injection in D-IIID *Nucl. Fusion* **55** 063018
[9] Scotti F. *et al* 2013 Core transport of lithium and carbon in ELM-free discharges with lithium wall conditioning in NSTX *Nucl. Fusion* **53** 083001
[10] Ruzic D.N., Xu W., Andruczyk D. and Jaworski M.A. 2011 Lithium-metal infused trenches (LiMIT) for heat removal in fusion devices *Nucl. Fusion* **51** 10200
[11] Shercliff J.A. 1979 Thermoelectric magnetohydrodynamics *J. Fluid Mech.* **91** 231–51
[12] Jaworski M.A., Gray T.K., Antonelli M., Kim J.J., Lau C.Y., Lee M.B., Neumann M.J., Xu W. and Ruzic D.N. 2010 Thermoelectric magnetohydrodynamic stirring of liquid metals *PRL* **104** 094503
[13] Xu W., Curreli D., Andruczyk D., Mui T., Switts R. and Ruzic D.N. 2013 Heat transfer of TEMHD driven lithium flow in stainless steel trenches *J. Nucl. Matter.* **438** S422
[14] Ren J., Hu J.S., Zuo G.Z., Sun Z., Li J.G., Ruzic D.N. and Zakharov L.E. 2014 First results of flowing liquid lithium limiter in HT-7 *Phys. Scr.* **T159** 014033
[15] de Groot B., Amad Z., Dahiya R.P., Engeln R., Goedheer W.J., Lopez Cardozo N.J. and Veremiyenko V. 2003 Magnum psi, a new linear plasma generator for plasma surface interaction studies in ITER relevant conditions *Fusion Eng. Des.* **66–68** 413–7
[16] Fiflis P., Press A., Xu W., Andruczyk D., Curreli D. and Ruzic D.N. 2014 Wetting properties of liquid lithium on select fusion relevant surfaces *Fusion Eng. Des.* 89 2827–32
[17] Djordjevic V.D. and Redekopp L.G. 1977 On 2D packets of capillary-gravity waves *J. Fluid Mech.* **79** 703–14
[18] Jung S., Andruczyk D. and Ruzic D.N. 2012 Laboratory investigation of vapor shielding for lithium-coated molybdenum in DeVeX *IEEE Trans. Plas. Sci.* **40** 730–4
[19] Jung S. 2014 Development of high energy pulsed plasma simulator for plasma-lithium trench experiment *Doctoral Thesis* UIUC
[20] ANSYS® Academic Research, FLUENT Release 15.0
[21] Whyte D.G., Evans T.E., Wong C.P.C., West W.P., Bastasz R., Allain J.P. and Brooks J.N. 2004 Experimental observations of lithium as a plasma-facing surface in the D-IIID tokamak divertor *Fusion Eng. Des.* **72** 133–47
[22] Jaworski M.A., Gerhardt S.P., Morley N.B., Abrams T., Kaita R., Kallman J., Kugel H., Majeski J. and Ruzic D.N. 2011 Macroscopic motion of liquid metal plasma facing components in a diverted plasma *J. Nucl. Mater.* **415** S985–8
[23] DeTemmerman G., van den Berg M.A., Scholten J., Lof A., van der Meiden H.J., van Eck H.J.N., Morgan T.W., de Kruijf T.M., Zeijlmans van Emmichoven P.A. and Zielinski J.J. 2012 High heat flux capabilities of the magnum-PSI linear plasma device *Fusion Eng. Des.* **88** 483–7